SERBIAN JOURNAL OF ELECTRICAL ENGINEERING
Vol. 11, No. 3, October 2014, 501-521

UDC: 621.313.333-253:519.853 **DOI: 10.2298/SJEE1403501S**

Observer Based Parallel IM Speed and Parameter Estimation

Saša Skoko[1], Darko Marčetić[1], Veran Vasić[1], Đura Oros[1]

Abstract: The detailed presentation of modern algorithm for the rotor speed estimation of an induction motor (IM) is shown. The algorithm includes parallel speed and resistance parameter estimation and allows a robust shaft-sensorless operation in diverse conditions, including full load and low speed operation with a large thermal drift. The direct connection between the injected electric signal in the d-axis and the component of injected rotor flux were pointed at. The algorithm that has been applied in the paper uses the extracted component of the injected rotor flux in the *d*-axis from the observer state vector and filtrated measured electricity of one motor phase. By applying the mentioned algorithm, the system converges towards the given reference.

Keywords: Induction motor, Luenberger observer, Parameter identification.

1 Introduction

The simple construction and superior exploitation characteristics have made the induction motor very popular in a wide range of industrial drive applications, from the unregulated pump and compressor facilities, to modern servomechanisms with the precise regulation of speed and position [1, 2]. Before the use of induction motors in regulated drives, the DC motors were used. However, the DC motors are more complex in their construction, affecting both the production price and the price of drive maintenance. The usage of the induction motor allows the reduction of both drive prices, as well as the minimization of electric energy losses, greater reliability, converter volume reduction, etc. Further advance and drive price reduction is possible, though it demands the field oriented control with minimum sensors needed for drive to operate. Until recently, in the field of the shaft-sensorless drives with an induction motor, simpler techniques of estimation are typically used, such as open-loop estimators and MRAS estimators [3]. The main purpose of these speed estimators is the online calculation of position and the amplitude of the selected machine state vector, such are stator, rotor or magnetizing flux vector. However, the open-loop machine model state calculation can be effected with

[1]Department of Power Electronics and Drives, Faculty of Technical Sciences, University of Novi Sad, Serbia
E-mails: sasaskoko78@gmail.com, darmar@uns.ac.rs, veranv@uns.ac.rs, orosd@uns.ac.rs

incorrect machine equivalent circuit parameters, the nonlinearity of voltage inverter transfer function and the errors in the stator current measurement or stator voltage estimation. As a consequence, all those solutions are unreliable during the low stator voltage operation and have limited speed range for the safe and robust operation ($f < 1$ Hz). Out of the above-given analysis, it can be concluded that the open-loop methods are not applicable in modern high performance drives with an induction motor. The needed improvement in the electrical machine flux estimation can be achieved only by using the linear flux observer, which is made more reliable and robust to machine parameter changes by the corrective state feedback [4]. The linear observer discussed in this paper is the Luenberger observer (LO). LO uses the rotor flux and the stator current vectors as two state variables and performs their stable simultaneous estimation in a wide speed range by arbitrary allocating the observer poles [5]. The rotational speed is estimated on the basis of the difference between the measured and the LO estimated stator current vector. This observer is similar to the MRAS observer structure, with the IM used as the reference model and the LO as the adjustable model. However, the LO rotor speed estimation represents an activity with a corrective feedback via the stator current error, while the MRAS estimates the rotor speed in the open loop manner. In [5] is shown that the Extended Luenberger observer (ELO) can be successfully used in the shaft-sensorless IM drive with the direct field orientation and operating with low rotational speeds. In this paper, the possibilities of the parallel estimation of the stator resistance and rotor speed, as well as limitations during the parallel estimation of rotor resistance and rotor speed are shown. Based on that analysis, the authors suggest a test signal based procedure for the estimation of the rotor resistance [6, 7]. Paper [8] presents an original method for the implementation of a sensorless indirect stator-flux oriented control of induction motor drives. The proposed control scheme in [8] has a good performance with the computational complexity reduction obtained by using the analytical relation to determine the LO gain matrix. In paper [9] different types of IM-VFDs are presented. The main focus in [9] is on the sensorless estimation techniques which are being applied to make IM-VFDs more effective during wide speed operations, including very-high and very-low speed regions. In paper [10] a nonlinear adaptive control algorithm is proposed for the IM. It is based on a two time-scale observer that allows the on-line identification of three critical uncertain parameters, i.e., load torque and motor stator and rotor resistances. This paper points out the basic equations following from the usage of the injected test signal in the *d*-axis of the stator current, and the synthesis algorithms that allow the convergence of the numerical model of a drive to the set value of the speed of rotation.

2 Mathematical Model of Induction Machine and Control Principle

The mathematical model of the induction machine consists of systems of differential and algebraic equations describing electromagnet and mechanical phenomena in a machine [11]. Fig. 1a shows the induction machine in an original phase domain, where indexes *a*, *b* and *c* present stator measures while indexes *A*, *B*, *C* present the indexes of rotor values. The angle between the *a* axis and the *A* axis is marked with ϑ.

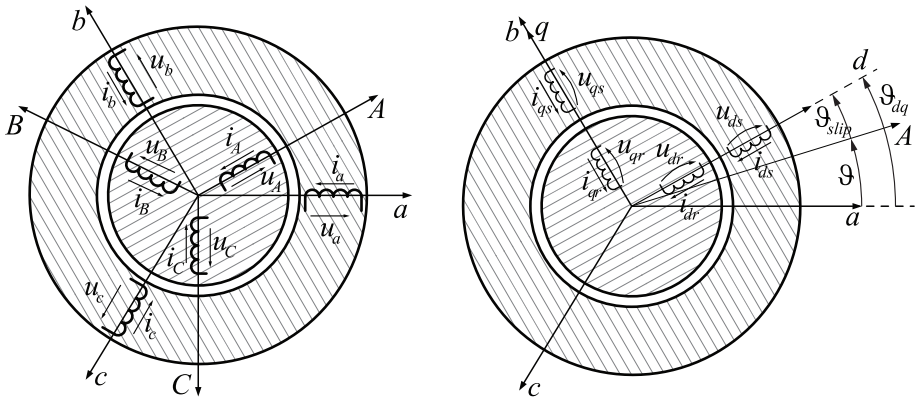

(a) (b)

Fig. 1 – (a) *Three phase induction motor in the original domain,*
(b) *Three phase induction motor in the dq domain.*

After the Clarke and Park transformations are applied onto the original phase domain model, one gets the machine model in the rotating axis *dq*-domain, Fig. 1b:

$$u_{ds} = R_s i_{ds} + \frac{\mathrm{d}\Psi_{ds}}{\mathrm{d}t} - \omega_{dq}\Psi_{qs}\,, \tag{1}$$

$$u_{qs} = R_s i_{qs} + \frac{\mathrm{d}\Psi_{qs}}{\mathrm{d}t} + \omega_{dq}\Psi_{ds}\,, \tag{2}$$

$$u_{dr} = R_r i_{dr} + \frac{\mathrm{d}\Psi_{dr}}{\mathrm{d}t} - (\omega_{dq} - \omega)\Psi_{qr}\,, \tag{3}$$

$$u_{qr} = R_r i_{qr} + \frac{\mathrm{d}\Psi_{qr}}{\mathrm{d}t} + (\omega_{dq} - \omega)\Psi_{dr}\,, \tag{4}$$

where:

ω_{dq} – electrical angle velocity of reference axes systems,

R_s, R_r – stator and rotor resistance,

u_{ds}, u_{qs} – stator voltages,

u_{dr}, u_{qr} – rotor voltages,

i_{ds}, i_{qs} – stator currents,

i_{dr}, i_{qr} – rotor currents,

Ψ_{ds}, Ψ_{qs} – stator fluxes,

Ψ_{dr}, Ψ_{qr} – rotor fluxes,

ω – motor angular velocity.

The model is completed with the algebraic equations:

$$\Psi_{ds} = L_s i_{ds} + L_m i_{dr}, \quad \Psi_{qs} = L_s i_{qs} + L_m i_{qr}, \tag{5}$$

$$\Psi_{dr} = L_r i_{dr} + L_m i_{ds}, \quad \Psi_{qr} = L_r i_{qr} + L_m i_{qs}. \tag{6}$$

where:

$L_s = L_{\gamma s} + L_m$, $L_r = L_{\gamma r} + L_m$ are stator and rotor self inductances,

L_m is mutual inductance,

$L_{\gamma s}, L_{\gamma r}$ are stator and rotor leakage inductances.

Finally, the motor torque can be calculated using the stator current and flux vector:

$$T_c = P(i_{qs}\Psi_{ds} - i_{ds}\Psi_{qs}), \tag{8}$$

where P is the number of pole pairs.

The angle between the rotor axis and the d-axis represents the rotor slip angle:

$$\vartheta_{slip} = \vartheta_{dq} - \vartheta, \tag{9}$$

where:

ϑ_{dq} is the position of dq reference system,

ϑ is the position of the rotor reference system (Fig. 1b).

In that case, the coordinates of the rotor axis and the rotating axis system are connected with the following equations:

$$\vartheta = \vartheta(0) + \int_0^t \omega \, \mathrm{d}t, \quad \vartheta_{dq} = \vartheta_{dq}(0) + \int_0^t \omega_{dq} \, \mathrm{d}t. \tag{10}$$

Both direct and indirect field orientation achieve the independent control of the torque and the flux of an induction motor. In the field orientation towards the rotor flux, the flux amplitude is controlled with the electric current component parallel to the rotor flux vector or the *d*-axis of the rotating coordinate system. In the same time the orthogonal component of the stator current vector controls the torque [12, 13]. In the case of the rotor flux orientation the following is valid:

$$\underline{\psi}_r = \psi_{dr}\,, \tag{11}$$

$$\underline{\psi}_{qr} = 0\,. \tag{12}$$

The standard indirect field orientation requires the rotor position data taken of the speed sensor. In that case the regulation structure must be fed with the proper rotor speed and position estimates. In Fig. 2, the principle scheme of the shaft-sensorless vector control of an induction motor with the rotor flux orientation is shown.

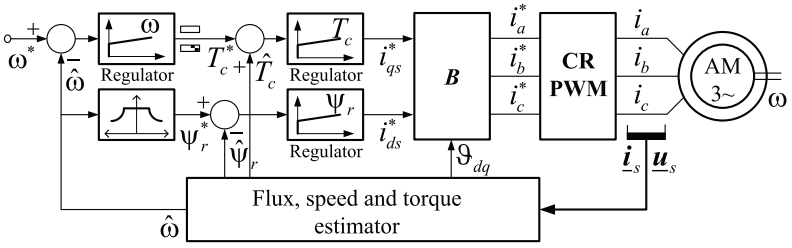

Fig. 2 – *Principle scheme of the vector controlled induction motor with an orientation in the direction of the rotor flux.*

3 Mathematical Model of Luenberger Observer

Full order Luenberger observer allows the rotor speed estimation of the induction motor. The observer basically represents the estimator with the state variable feedback and enables the estimation of state variables and/or parameters of a nonlinear dynamic system in real time. In the case of the induction motor, the Luenberger observer is constructed with the stator current and the rotor flux vectors as state variables. The Luenberger observer is based on the induction motor model in the stationary reference frame, equations (1) – (6), where $\omega_{dq} = 0$. In a shortened form, the state space model can be written as follows:

$$\frac{\mathrm{d}}{\mathrm{d}t}\boldsymbol{x} = \boldsymbol{A}\boldsymbol{x} + \boldsymbol{B}\boldsymbol{u}_s\,, \tag{13}$$

$$\boldsymbol{y} = \boldsymbol{C}\boldsymbol{x}\,, \tag{14}$$

where:

$\boldsymbol{x}$ – vector of the observer state,

$\boldsymbol{u}_s$ – the observer input vector,

$\boldsymbol{y}$ – the observer output vector,

$\boldsymbol{A}$ – state matrix of the observer (Appendix A),

$\boldsymbol{B}$ – input matrix of the observer,

$\boldsymbol{C}$ – output matrix of the observer.

$$\boldsymbol{x} = \begin{bmatrix} i_{\alpha s} & i_{\beta s} & \psi_{\alpha r} & \psi_{\beta r} \end{bmatrix}^{\mathrm{T}}, \tag{15}$$

$$\boldsymbol{u_s} = \begin{bmatrix} u_{\alpha s} & u_{\beta s} & 0 & 0 \end{bmatrix}^{\mathrm{T}}, \tag{16}$$

$$\boldsymbol{y} = \begin{bmatrix} i_{\alpha s} & i_{\beta s} \end{bmatrix}^{\mathrm{T}}. \tag{17}$$

The matrices $\boldsymbol{B}$ and $\boldsymbol{C}$ are defined as follows:

$$\boldsymbol{B} = \begin{bmatrix} \dfrac{1}{L_s'} & 0 & 0 & 0 \\ 0 & \dfrac{1}{L_s'} & 0 & 0 \end{bmatrix}^{\mathrm{T}}, \quad \boldsymbol{C} = \begin{bmatrix} 1 & 0 & 0 & 0 \\ 0 & 1 & 0 & 0 \end{bmatrix}.$$

The modified form of the Luenberger observer is defined with the equations (18) and (19) and it is called the Extended Luenberger Observer (ELO).

$$\frac{\mathrm{d}}{\mathrm{d}t}\hat{\boldsymbol{x}} = \hat{\boldsymbol{A}}\hat{\boldsymbol{x}} + \boldsymbol{B}\boldsymbol{u} + \boldsymbol{G}(\hat{\boldsymbol{i}}_s - \boldsymbol{i}_s), \tag{18}$$

$$\hat{\boldsymbol{i}}_s = \boldsymbol{C}\hat{\boldsymbol{x}}. \tag{19}$$

The gain matrix of the Luenberger observer is defined as follows:

$$\boldsymbol{G} = \begin{bmatrix} g_1\boldsymbol{I} + g_2\boldsymbol{J} \\ g_3\boldsymbol{I} + g_4\boldsymbol{J} \end{bmatrix} = \begin{bmatrix} \boldsymbol{G}_1 \\ \boldsymbol{G}_2 \end{bmatrix}, \quad \boldsymbol{I} = \begin{bmatrix} 1 & 0 \\ 0 & 1 \end{bmatrix}, \quad \boldsymbol{J} = \begin{bmatrix} 0 & -1 \\ 1 & 0 \end{bmatrix}.$$

The elements of the gain matrix $\boldsymbol{G}$ are defined as:

$$g_1 = (k-1)(a_{r11} + a_{r22}),$$

$$g_2 = (k-1)a_{i22},$$

$$g_3 = (k^2-1)(ca_{r11} + a_{r22}) - c(k-1)(a_{r11} + a_{r22}),$$

$$g_4 = -c(k-1)a_{i22}.$$

where the coefficients $a_{r11}, a_{r12}, a_{i12}, a_{r21}, a_{r22}, a_{i22}$ are defined in Appendix F. In Fig. 3, the principle scheme of the Extended Luenberger Observer defined by (18) and (19) is shown.

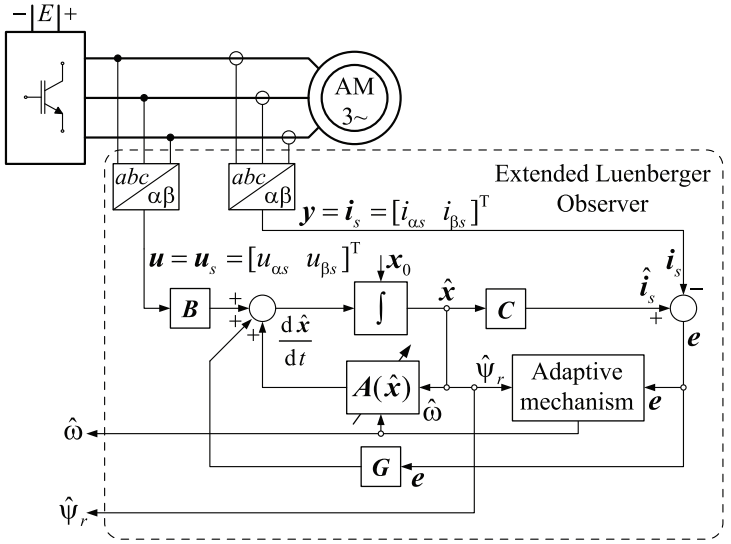

Fig. 3 – *Principle scheme of the Extended Luenberger Observer.*

4 Algorithm Synthesis for the Rotational Speed Estimation ($\hat{\omega}$)

The state space models describing the induction motor and the observer are given in (20) and (21).

$$\frac{\mathrm{d}\boldsymbol{x}}{\mathrm{d}t} = \boldsymbol{A}\boldsymbol{x} + \boldsymbol{B}\boldsymbol{u}_s, \quad \boldsymbol{i}_s = \boldsymbol{C}\boldsymbol{x}, \tag{20}$$

$$\frac{\mathrm{d}\hat{\boldsymbol{x}}}{\mathrm{d}t} = \hat{\boldsymbol{A}}\hat{\boldsymbol{x}} + \boldsymbol{B}\boldsymbol{u}_s + \boldsymbol{G}(\hat{\boldsymbol{i}}_s - \boldsymbol{i}_s), \quad \hat{\boldsymbol{i}}_s = \boldsymbol{C}\hat{\boldsymbol{x}}. \tag{21}$$

Vectors in (21) marked with '^' represent the estimated values. The error signal is defined as the difference between the actual and the estimated value $\boldsymbol{e} = (\boldsymbol{x} - \hat{\boldsymbol{x}})$. The first order derivative of the error signal is defined as, $\frac{\mathrm{d}\boldsymbol{e}}{\mathrm{d}t} = \frac{\mathrm{d}\boldsymbol{x}}{\mathrm{d}t} - \frac{\mathrm{d}\hat{\boldsymbol{x}}}{\mathrm{d}t}$, leading to,

$$\frac{\mathrm{d}\boldsymbol{e}}{\mathrm{d}t} = (\boldsymbol{A} + \boldsymbol{G}\boldsymbol{C})(\boldsymbol{x} - \hat{\boldsymbol{x}}) - (\hat{\boldsymbol{A}} - \boldsymbol{A})\hat{\boldsymbol{x}} = (\boldsymbol{A} + \boldsymbol{G}\boldsymbol{C})\boldsymbol{e} - \Delta\boldsymbol{A}\hat{\boldsymbol{x}}. \tag{22}$$

The induction motor speed estimation within the ELO can be defined using the Lyapunov criterion function $V(\boldsymbol{e}) = \boldsymbol{e}^{\mathrm{T}}\boldsymbol{e} + \dfrac{(\hat{\omega}-\omega)^2}{\lambda}$, where λ is the positive constant. Using (22), the first order derivative of the criterion function results in the following:

$$\frac{\mathrm{d}V}{\mathrm{d}t} = \boldsymbol{e}^{\mathrm{T}}\left[(\boldsymbol{A}+\boldsymbol{GC})^{\mathrm{T}} + (\boldsymbol{A}+\boldsymbol{GC})\right]\boldsymbol{e} - \hat{\boldsymbol{x}}^{\mathrm{T}}\Delta\boldsymbol{A}^{\mathrm{T}}\boldsymbol{e} - \boldsymbol{e}^{\mathrm{T}}\Delta\boldsymbol{A}\hat{\boldsymbol{x}} + \frac{2\Delta\omega}{\lambda}\frac{\mathrm{d}\hat{\omega}}{\mathrm{d}t}. \quad (23)$$

The condition of the asymptotic stability is fulfilled if the sum of the second, the third and the fourth term in (23) equals 0

$$0 = -\hat{\boldsymbol{x}}^{\mathrm{T}}\Delta\boldsymbol{A}^{\mathrm{T}}\boldsymbol{e} - \boldsymbol{e}^{\mathrm{T}}\Delta\boldsymbol{A}\hat{\boldsymbol{x}} + \frac{2\Delta\omega}{\lambda}\frac{\mathrm{d}\hat{\omega}}{\mathrm{d}t} \quad (24)$$

The solution of the equation (24) exposes the method for the induction motor rotor speed estimation:

$$\hat{\omega} = \int \frac{\lambda}{c}(\hat{\psi}_{\beta r}\boldsymbol{e}_{i\alpha s} - \hat{\psi}_{\alpha r}\boldsymbol{e}_{i\beta s})\,\mathrm{d}t\,. \quad (25)$$

The speed estimation method used by the ELO estimated rotor flux vector and the error between the measured and by the ELO estimated current vector. The coefficient c is defined as $c = \dfrac{L_s' L_r}{L_m}$, where λ represents the positive constant number. The appropriate adaptive mechanism is embodied in the diagram in the Fig. 4.

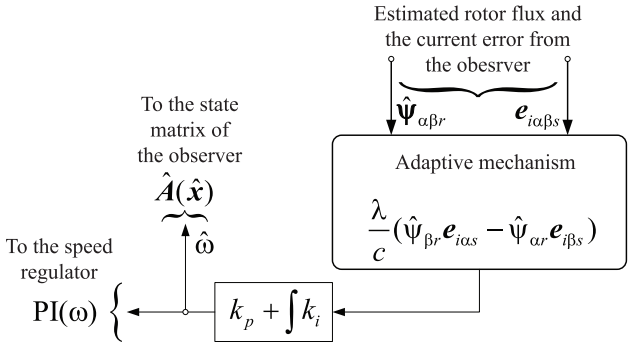

Fig. 4 – *The block diagram of the adaptive mechanism for the rotational speed estimation of the motor.*

The effectiveness of the ELO speed estimation is tested using computer simulations and results provided in Fig. 5. Different speed profiles are used. After no load start, the different load is applied in the 1st, 2nd and 3rd second,

with the load torque of 0.5 pu, 0.8 pu and 1 pu, respectively, where the nominal torque is 50 Nm.

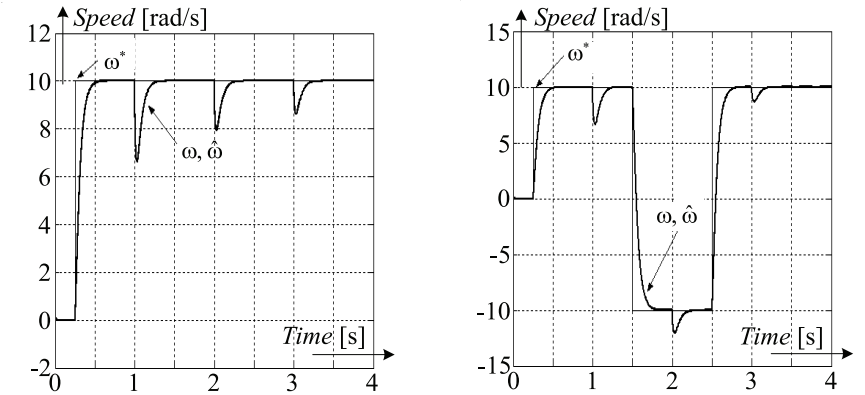

Fig. 5 – (a) *Change of the real and the estimated speed for the given testing conditions,* (b) *Change of the real and the estimated speed with a sudden reverse to* –10 rad/s *and a quick return to* 10 rad/s.

As results show, the ELO is capable of tracking the rotor speed under the diverse test conditions. However, the given speed estimation algorithm does not include the discrepancy between the motor and the observer parameters. If parameters used by the observer are not correct, there is a deviation between the actual and the estimated motor speed, as the next set of simulation results show (Fig. 6).

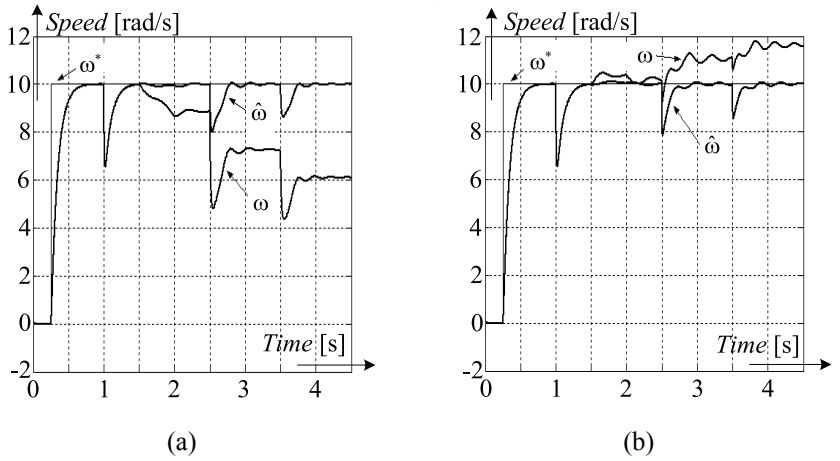

Fig. 6 – (a) *Change of the estimated and the real motor speed for* $R_{sm} = 1.2R_s$, (b) *Change of the estimated and the real motor speed for* $R_{sm} = 0.8R_s$.

The referent speed was set to $\omega^* = 10$ rad/s. The motor was first started without the load, and the load was applied in the 1st, 2.5th and 3.5th second, 0.5 pu, 0.8 pu and 1 pu, respectively, where the nominal torque is 50 Nm. The stator (rotor) resistance is changed linearly in the motor model by ±20% during the 1.5 s – 2 s period.

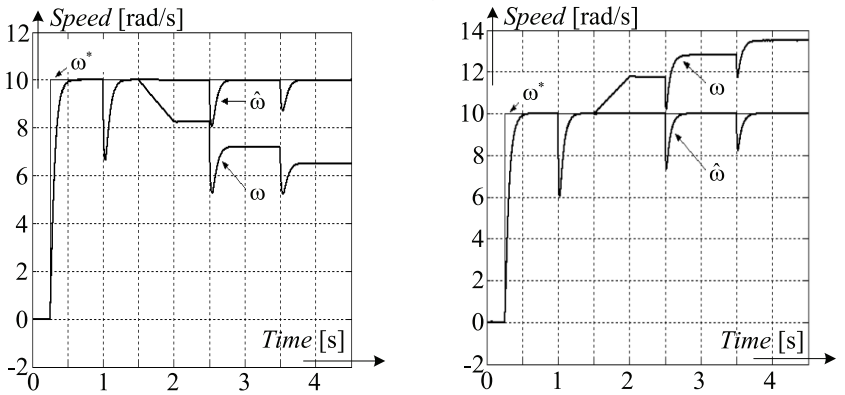

Fig. 7 – (a) *Change of the estimated and the real motor speed for* $R_{rm} = 1.2R_r$*;* (b) *Change of the estimated and the real motor speed for* $R_{rm} = 0.8R_r$.

The results show that the change in the stator resistance influences both the speed estimation and the flux vector orientation. The rotor resistance changes results in the estimated speed error as well; however, contrary to the stator resistance, it does not influence the rotor flux vector orientation [6].

4.1 Mathematical algorithm synthesis for the parallel estimation R_s and $\hat{\omega}$

The algorithm for the parallel estimation of the rotor speed and the motor stator resistance can be constructed using the Lyapunov function $V(\boldsymbol{e}) = \boldsymbol{e}^{\mathrm{T}}\boldsymbol{e} + \dfrac{(\hat{R}_s - R_s)^2}{\lambda}$. Using the same procedure as before, the mechanism for the parallel stator resistance estimation is as follows:

$$\frac{\mathrm{d}\hat{R}_s}{\mathrm{d}t} = -\frac{\lambda}{L'_s}(\hat{i}_{\alpha s}\boldsymbol{e}_{i\alpha s} + \hat{i}_{\beta s}\boldsymbol{e}_{i\beta s}) = -\lambda_1(\hat{i}_{\alpha s}\boldsymbol{e}_{i\alpha s} + \hat{i}_{\beta s}\boldsymbol{e}_{i\beta s}). \tag{26}$$

Similar as the rotor speed, the stator resistance can be estimated by using the ELO estimated stator current vector and the error between the actual and the estimated stator current vector. The simulation results showing the efficiency of the additional identification of the stator resistance are given in Fig. 8. The algorithm for the additional stator resistance identification was active during

this set of computer simulations. The stator resistance in the induction motor model is linear and it changes linearly $R_{sm} = \pm 20\% R_s$ in the time period between 1.5 s and 2 s. The speed is set to a relatively low value of $\omega^* = 10$ rad/s and the motor is loaded in the 1 s, 2.5 s and 3.5 s, with the torque of 0.5 pu, 0.8 pu and 1 pu, respectively, where the nominal torque is 50 Nm.

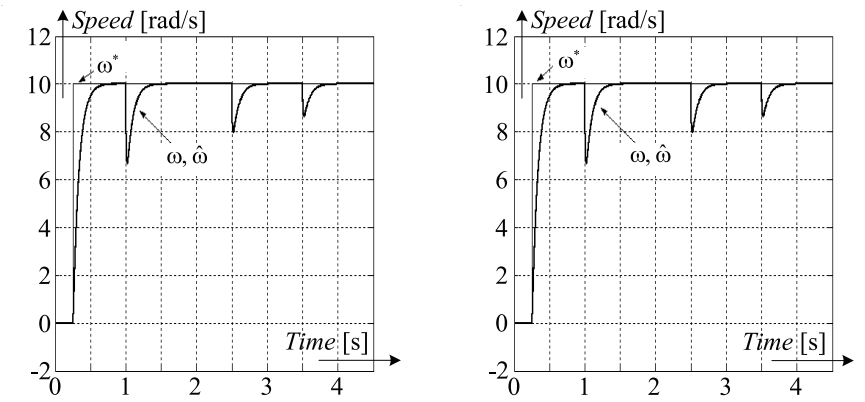

(a) (b)

Fig. 8 – (a) *Speed change of the rotor* $\omega^*, \omega, \hat{\omega} = f(t)$ *for* $R_{sm} = 1.2R_s$ *with the correction* R_s*;*
(b) *Speed change of the rotor* $\omega^*, \omega, \hat{\omega} = f(t)$ *for* $R_{sm} = 0.8R_s$ *with the correction* R_s*.*

4.2 Mathematical algorithm synthesis for the parallel estimation R_r and $\hat{\omega}$

Applying the basic Lyapunov criterion function on the rotor resistance results in the following $V(\boldsymbol{e}) = \boldsymbol{e}^{\mathrm{T}}\boldsymbol{e} + \dfrac{(\hat{R}_r - R_r)^2}{\lambda}$ As the result, the formula for the rotor time constant ($T_r = L_r / R_r$) identification is given,

$$\frac{\mathrm{d}}{\mathrm{d}t}\left(\frac{1}{\hat{T}_r}\right) = \frac{\lambda_2}{L_r}\left[(\hat{\psi}_{\alpha r} - L_m \hat{i}_{\alpha s})\boldsymbol{e}_{i\alpha s} + (\hat{\psi}_{\beta r} - L_m \hat{i}_{\beta s})\boldsymbol{e}_{i\beta s}\right] . \tag{27}$$

The effectiveness of (27) was tested via computer simulations and results are given in Fig. 9, with the same load conditions and speed reference as in Fig. 8.

The obtained results show that the ELO with the parallel estimation of the speed and rotor time constant cannot operate [5, 6]. The only manner to do that is to create the change in the rotor flux vector, which results in the non-zero right side of (27). The possibility for the parallel speed and rotor circuit parameter estimation will be further explored in the next chapter.

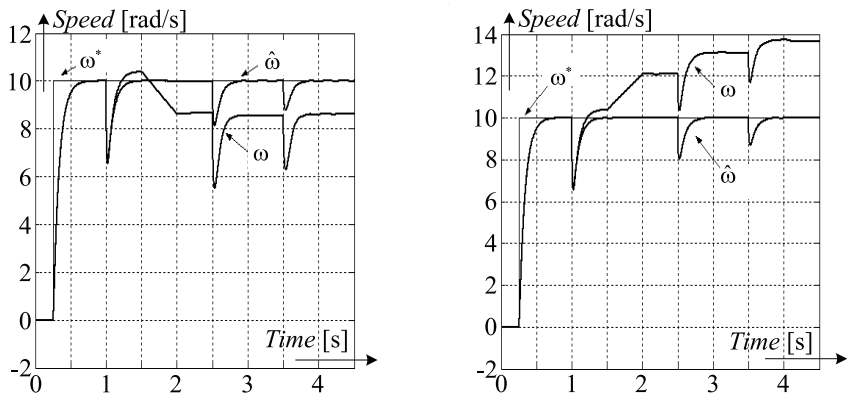

(a) (b)

Fig. 9 – (a) *Speed change of the rotor* $\omega^*, \omega, \hat{\omega} = f(t)$ *for* $R_{rm} = 1.2R_r$ *with the correction* R_r*;*
(b) *Speed change of the rotor* $\omega^*, \omega, \hat{\omega} = f(t)$ *for* $R_{rm} = 0.8R_r$ *with the correction* R_r*.*

5 R_r (T_r) Estimation on the Basis of the Injected Test Signal

Steady state equations of the induction motor show that it is impossible to estimate the rotor speed and rotor resistance in parallel. That parallel estimation is possible only if non-zero rate of the change in the rotor flux vector is created. One manner to do that is to inject the test signal in the *d*-axis. The usage of the injected signal in the *d*-axis is already an established procedure, applied in a numerous number of papers. In this section the connection between the injected electric signal i_{ds}^i and the resulting flux component ψ_{dr}^i is investigated first. The non-linear induction motor model

$$\frac{\mathrm{d}}{\mathrm{d}t}\begin{bmatrix}\Psi_{dr}\\ \Psi_{qr}\end{bmatrix} = \begin{bmatrix}\frac{L_m}{T_r} & 0\\ 0 & \frac{L_m}{T_r}\end{bmatrix}\cdot\begin{bmatrix}i_{ds}\\ i_{qs}\end{bmatrix} - \begin{bmatrix}\frac{1}{T_r} & 0\\ 0 & \frac{1}{T_r}\end{bmatrix}\cdot\begin{bmatrix}\Psi_{dr}\\ \Psi_{qr}\end{bmatrix} + \omega_{sl}\begin{bmatrix}0 & 1\\ -1 & 0\end{bmatrix}\cdot\begin{bmatrix}\Psi_{dr}\\ \Psi_{qr}\end{bmatrix},$$

is fed by signals that have the steady state value and the small signal deviations around their steady state value, as presented

$$\Psi_{dr} = \Psi_{dr}^o + \Delta\Psi_{dr}, \quad \Psi_{qr} = \Psi_{qr}^o + \Delta\Psi_{qr},$$

$$i_{ds} = i_{ds}^o + \Delta i_{ds}, \quad i_{qs} = i_{qs}^o + \Delta i_{qs},$$

$$\omega_{sl} = \omega_{sl}^o + \Delta\omega_{sl}\ .$$

where the x^o_{dq} marks the steady state value of the signal and the Δx_{dq} represents the small signal. After steady state equations are subtracted, the small signal model of the induction motor can be constructed as follows:

$$\frac{\mathrm{d}}{\mathrm{d}t}(\Delta\Psi_{dr}) + \frac{1}{T_r}\Delta\Psi_{dr} - \omega^o_{sl}\Delta\Psi_{qr} - \Delta\omega_{sl}\Psi^o_{qr} = \frac{L_m}{T_r}\Delta i_{ds}, \tag{28}$$

$$\frac{\mathrm{d}}{\mathrm{d}t}(\Delta\Psi_{qr}) + \frac{1}{T_r}\Delta\Psi_{qr} + \omega^o_{sl}\Delta\Psi_{dr} + \Delta\omega_{sl}\Psi^o_{dr} = \frac{L_m}{T_r}\Delta i_{qs}\ . \tag{29}$$

The small signal model is valid for a given steady state point, defined by ω^o_{sl}, Ψ^o_{dr} and Ψ^o_{qr}. The small signal model shows how a small signal in the *d*-axis current component Δi_{ds} generates the change in the motor flux in the *d*-axis, the small signal $\Delta\Psi_{dr}$. The connection between the injected components i^i_{ds} and Ψ^i_{dr} is defined by the following relation:

$$\frac{\mathrm{d}}{\mathrm{d}t}(\Delta\Psi_{dr}) + \frac{1}{T_r}\Delta\Psi_{dr} = \frac{L_m}{T_r}\Delta i_{ds}\text{, respectively } \frac{\mathrm{d}}{\mathrm{d}t}(\Psi^i_{dr}) + \frac{1}{T_r}\Psi^i_{dr} = \frac{L_m}{T_r}i^i_{ds}, \tag{30}$$

while $i^i_{ds} = \Delta i_{ds}$ and $\Psi^i_{dr} = \Delta\Psi_{dr}$. If the periodic signal is injected into the *d*-axis stator current (i^i_{ds}), $i^i_{ds} = I^i \sin\omega^i t = 0{,}1 i_{dsn}\sin\omega^i t$ the signal created in the *d*-axis rotor flux component is:

$$\begin{aligned}\Psi_{dr} = &\left(\frac{L_m I^i T_r \omega^i}{T_r^2\omega^{i2}+1} - L_m i^o_{ds}\right)e^{-\frac{t}{Tr}} + L_m i^o_{ds} + \\ &+\left(L_m I^i - \frac{L_m I^i T_r^2 \omega^{i2}}{T_r^2\omega^{i2}+1}\right)\sin\omega^i t - \frac{L_m I^i T_r \omega^i}{T_r^2\omega^{i2}+1}\cos\omega^i t.\end{aligned} \tag{31}$$

The third and the fourth part of the equation (31) are the components of the injected flux Ψ^i_{dr}. During the simulations, the amplitude of the injected test signal is set to 10% of the nominal *d* axis stator current while its frequency is set to 250 Hz. The vector diagram showing the small signal stator currents and the corresponding small signal in the *d*-axis rotor flux is given in Fig. 10. The suggested rotor time constant parameter correction algorithm is given in the following relation:

$$\hat{T}_r = \frac{L_m i^i_{ds} - \hat{\psi}^i_{dr}}{\frac{\mathrm{d}}{\mathrm{d}t}(\hat{\psi}^i_{dr})}, \quad \text{or} \quad \hat{R}_r = \frac{L_r \frac{\mathrm{d}}{\mathrm{d}t}(\hat{\psi}^i_{dr})}{L_m i^i_{ds} - \hat{\psi}^i_{dr}}. \tag{32}$$

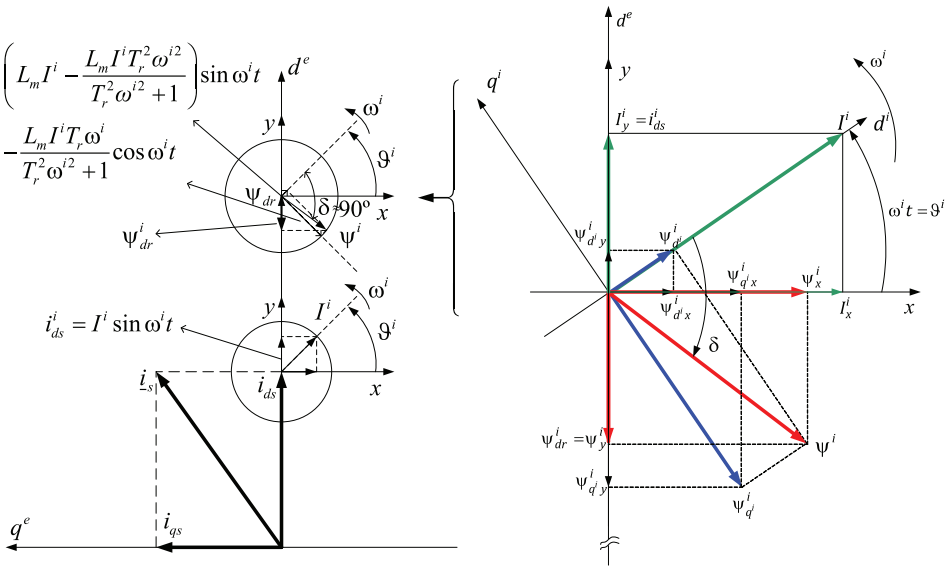

Fig. 10 – *Vector diagram of the injected current and the resulting d-axis flux with the appropriate components.*

Fig. 10 shows the injected current I^i and the corresponding injected flux Ψ^i, which comes from the injected current, with the appropriate components in the auxiliary coordinate systems (d^i, q^i – auxiliary coordinate system of the injected current, x, y – auxiliary coordinate system of the corresponding injected flux). The stator electric current i_{ds}^i used in the equation (32) can be filtered from the measured stator current, while the used $\hat{\Psi}_{dr}^i$ can be filtered from the estimated rotor flux in the observer. The rotor time constant identification method, which can be applied in parallel with the speed estimation, is shown in the next figure.

The block diagram of the Luenberger observer with the parallel algorithm for the rotor resistance correction is shown in Fig. 12.

Matrix $\boldsymbol{C}_1$ is defined in Appendix G. The effectiveness of the parallel rotor speed and the rotor circuit parameter estimation is tested via computer simulations, Fig. 13. The mechanism for the additional identification of the rotor resistance and the rotor time constant is activated at 2.1 s of the simulation time. In the time period 1.5–2.5 s, the rotor resistance in the motor model is changed linearly to ±20% from its nominal value. The motor magnetization is undertaken and the loading is done at 1 s, 2.5 s and 3.8 s, with the load torque of 0.5 pu, 0.8 pu and 1 pu, respectively, where the nominal torque is 50 Nm.

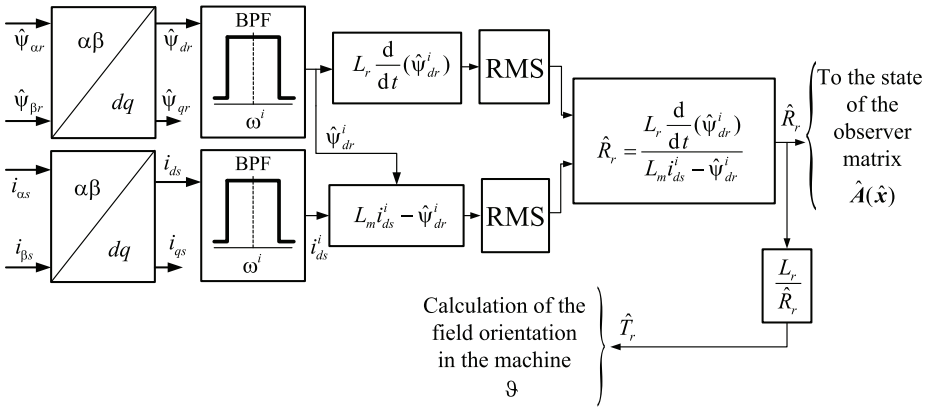

Fig. 11 – *Block diagram of the correctional algorithm for the independent estimation R_r (T_r), based on the injected test signal.*

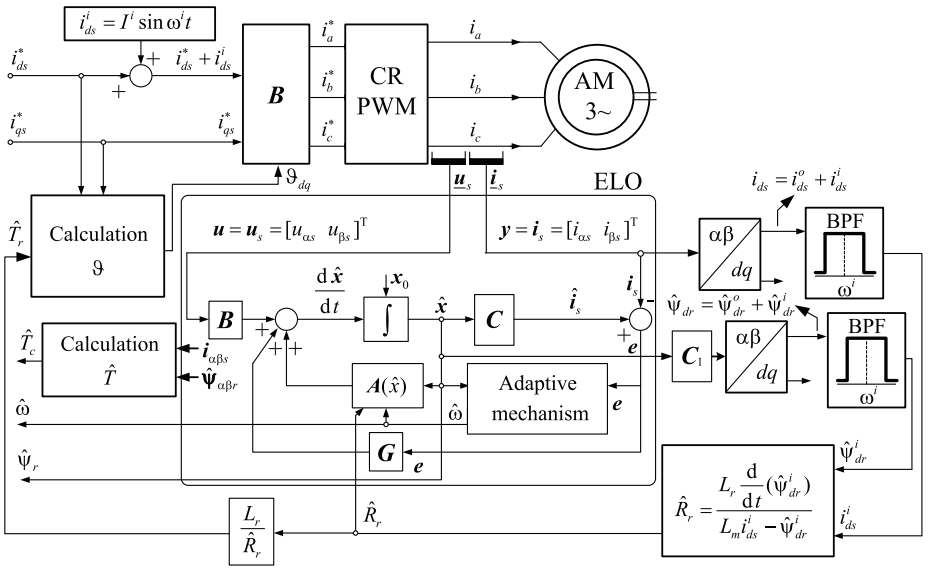

Fig. 12 – *Principal block diagram of the correctional algorithm synthesis for the independent estimation of the algorithm R_r (T_r) and the observer.*

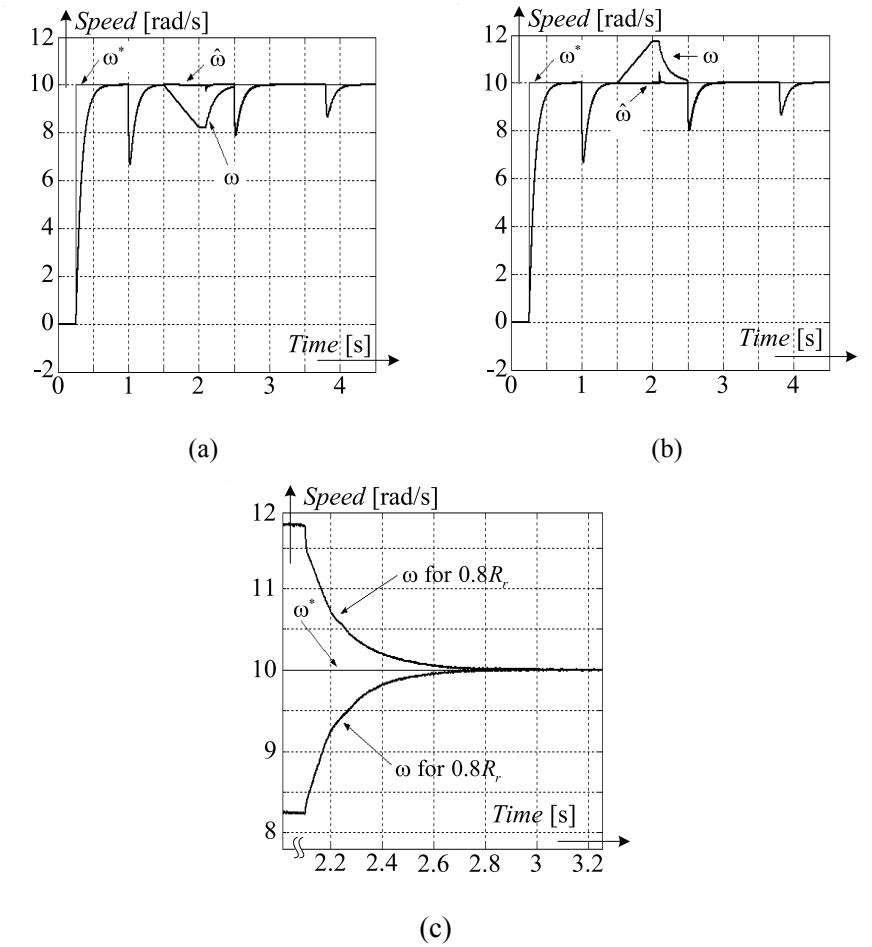

Fig. 13 – (a) *Change of* $\omega^*, \omega, \hat{\omega} = f(t)$ *for the case* $R_{rm} = 1.2R_r$;
(b) *Change of* $\omega^*, \omega, \hat{\omega} = f(t)$ *for the case* $R_{rm} = 0.8R_r$;
(c) *Change of* $\omega^*, \omega = f(t)$ *for the case* $R_{rm} = \pm 20\%\ R_r$.

The final part shows the results of testing the model with the applied correction algorithm, which operates in parallel with the algorithm for estimating the rotor resistance. The system was tested for four characteristic sequences. Figs. 14 and 15 show the simulation results with the algorithm for the additional identification R_r (T_r) immediately activated. In the period between 1.5 s and 2.1 s, the value of the resistance in the motor model is changed linearly by +20%, compared to its nominal value. The motor magnetization is undertaken and the loading is done at 1 s, 2.6 s and 3.8 s, with the load torque of 0.5 pu, 0.8 pu and 1 pu, respectively, where the nominal torque is 50 Nm.

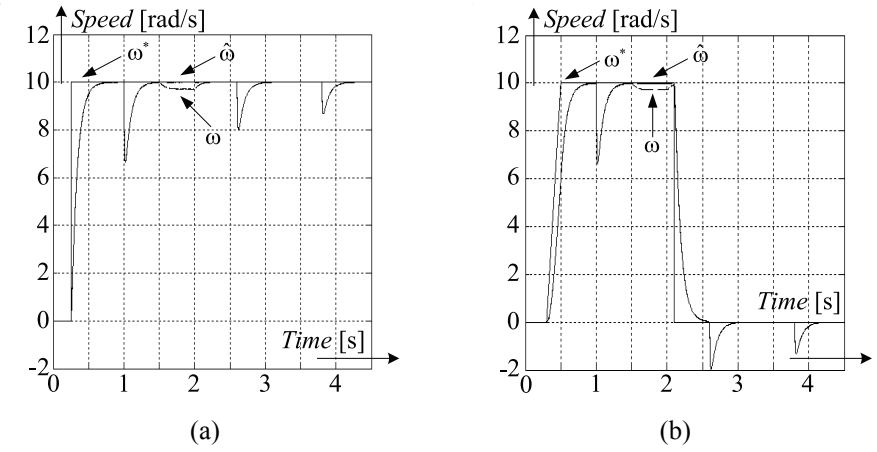

Fig. 14 – (a) *Change of* $\omega^*, \omega, \hat{\omega} = f(t)$ *for the case* $R_{rm}=1.2R_r$ (1st *sequence*), (b) *Change of* $\omega^*, \omega, \hat{\omega} = f(t)$ *for the case* $R_{rm}=1.2R_r$ (2nd *sequence*).

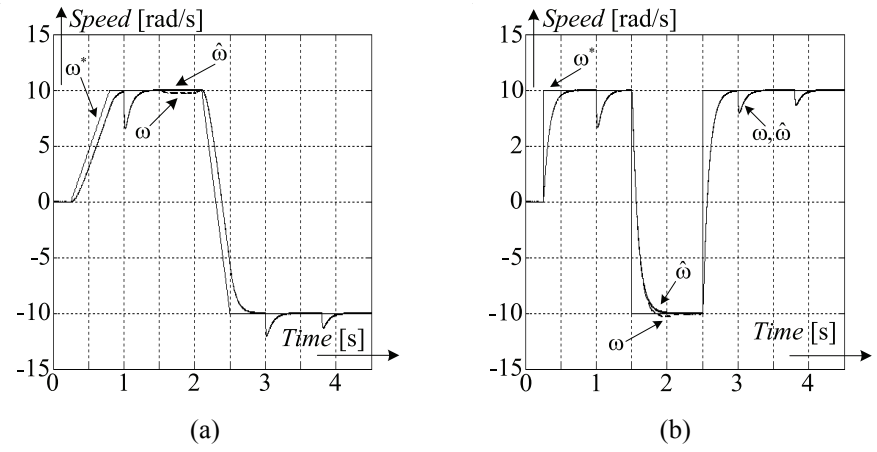

Fig. 15 – (a) *Change of* $\omega^*, \omega, \hat{\omega} = f(t)$ *for the case* $R_{rm} = 1.2R_r$ (3rd *sequence*); (b) *Change of* $\omega^*, \omega, \hat{\omega} = f(t)$ *for the case* $R_{rm} = 1.2R_r$ (4th *sequence*).

7 Conclusion

In the paper, the Luenberger observer based algorithm for the induction motor speed estimation is investigated. It has been shown that the basic Luenberger observer is sensitive to the change in both stator and rotor resistance parameters. In order to identify the algorithm that is more robust and satisfactory, the basic Luenberger observer is upgraded with the parallel stator and rotor resistance identification mechanism. The special attention is given to the parallel rotor resistance estimation which requires the injection of the test

signal in the stator current in the *d*-axis of the rotor flux. The direct link between the injected current test signal and the created small signal in the rotor flux is provided. As a result of that connection, the rotor resistance parameter corrective mechanism that can work in parallel with the speed estimation is suggested. The simulation results prove the effectiveness of the Luenberger speed observer upgraded in that manner. For any condition tested, it is shown that the rotor parameter value will converge towards the actual parameter value and that error in the estimated rotor speed will be cancelled. The only drawback of this algorithm can be in the intensive numeric calculations needed. One practical solution for that is to separate the rotor speed and the parameter estimation mechanisms by executing the second one with much slower rate. That would not affect the tracking of the slow changing motor parameter, but would save the significant amount of the processor time.

8 Acknowledgment

This work was supported in part by the Ministry of education and science of the Republic of Serbia within the project III 42004.

9 Appendices

Motor parameters used in the paper:

Manuf. code: 1.ZK 132 M4, Poles 4, Power 7.5 [kW],

R_s =2.044[Ω], R_r = 1.873[Ω],

L_s =0.1995 [H], L_r =0.2006 [H], L_m =0.1914 [H],

J =0.021 [kgm^2].

9.1 Appendix A

State matrix of the observer $\boldsymbol{A}$:

$$\boldsymbol{A}=\begin{bmatrix} -\dfrac{R_s L_r^2 + R_r L_m^2}{L_s' L_r^2} & 0 & \dfrac{L_m R_r}{L_s' L_r^2} & \omega\dfrac{L_m}{L_s' L_r} \\ 0 & -\dfrac{R_s L_r^2 + R_r L_m^2}{L_s' L_r^2} & -\omega\dfrac{L_m}{L_s' L_r} & \dfrac{L_m R_r}{L_s' L_r^2} \\ \dfrac{R_r L_m}{L_r} & 0 & -\dfrac{R_r}{L_r} & -\omega \\ 0 & \dfrac{R_r L_m}{L_r} & \omega & -\dfrac{R_r}{L_r} \end{bmatrix}.$$

9.2 Appendix B

State matrix of the observer $\hat{\boldsymbol{A}}$:

$$\hat{\boldsymbol{A}}=\begin{bmatrix} -\dfrac{R_s L_r^2+R_r L_m^2}{L_s' L_r^2} & 0 & \dfrac{L_m R_r}{L_s' L_r^2} & \hat{\omega}\dfrac{L_m}{L_s' L_r} \\ 0 & -\dfrac{R_s L_r^2+R_r L_m^2}{L_s' L_r^2} & -\hat{\omega}\dfrac{L_m}{L_s' L_r} & \dfrac{L_m R_r}{L_s' L_r^2} \\ \dfrac{R_r L_m}{L_r} & 0 & -\dfrac{R_r}{L_r} & -\hat{\omega} \\ 0 & \dfrac{R_r L_m}{L_r} & \hat{\omega} & -\dfrac{R_r}{L_r} \end{bmatrix}.$$

9.3 Appendix C

Matrix to determine the algorithm to estimate speed $\Delta\boldsymbol{A}=\hat{\boldsymbol{A}}-\boldsymbol{A}\Big|_{\omega}$:

$$\Delta\boldsymbol{A}=\begin{bmatrix} 0 & 0 & 0 & +\dfrac{\hat{\omega}-\omega}{c} \\ 0 & 0 & -\dfrac{\hat{\omega}-\omega}{c} & 0 \\ 0 & 0 & 0 & -(\hat{\omega}-\omega) \\ 0 & 0 & +(\hat{\omega}-\omega) & 0 \end{bmatrix}.$$

9.4 Appendix D

Matrix to determine the algorithm to estimate stator resistance $\Delta\boldsymbol{A}=\hat{\boldsymbol{A}}-\boldsymbol{A}\Big|_{R_s}$:

$$\Delta\boldsymbol{A}\Big|_{Rs}=\hat{\boldsymbol{A}}-\boldsymbol{A}=\begin{bmatrix} \dfrac{(R_s-\hat{R}_s)L_r^2}{L_s' L_r^2} & 0 & 0 & 0 \\ 0 & \dfrac{(R_s-\hat{R}_s)L_r^2}{L_s' L_r^2} & 0 & 0 \\ 0 & 0 & 0 & 0 \\ 0 & 0 & 0 & 0 \end{bmatrix}.$$

9.5 Appendix E

Matrix to determine the algorithm to estimate rotor resistance $\Delta \boldsymbol{A} = \hat{\boldsymbol{A}} - \boldsymbol{A}\big|_{R_r}$:

$$\Delta \boldsymbol{A}\big|_{Rr} = \hat{\boldsymbol{A}} - \boldsymbol{A} = \begin{bmatrix} -\dfrac{(\hat{R}_r - R_r)L_m^2}{L_s' L_r^2} & 0 & \dfrac{(\hat{R}_r - R_r)L_m}{L_s' L_r^2} & 0 \\ 0 & -\dfrac{(\hat{R}_r - R_r)L_m^2}{L_s' L_r^2} & 0 & \dfrac{(\hat{R}_r - R_r)L_m}{L_s' L_r^2} \\ \dfrac{(\hat{R}_r - R_r)L_m}{L_r} & 0 & -\dfrac{(\hat{R}_r - R_r)}{L_r} & 0 \\ 0 & \dfrac{(\hat{R}_r - R_r)L_m}{L_r} & 0 & -\dfrac{(\hat{R}_r - R_r)}{L_r} \end{bmatrix}.$$

9.6 Appendix F

Coefficients: $a_{r11}, a_{r12}, a_{i12}, a_{r21}, a_{r22}, a_{i22}$:

$$a_{r11} = -\frac{R_s L_r^2 + R_r L_m^2}{L_s' L_r^2}, \quad a_{r12} = \frac{L_m R_r}{L' L_r^2}, \quad a_{i12} = -\frac{L_m}{L' L_r}\omega,$$

$$a_{r21} = \frac{R_r L_m}{L_r}, \quad a_{r22} = -\frac{R_r}{T_r}, \quad a_{i22} = \omega.$$

9.7 Appendix G

Matrix $\boldsymbol{C}_1$:

$$\boldsymbol{C}_1 = \begin{bmatrix} 0 & 0 & 1 & 0 \\ 0 & 0 & 0 & 1 \end{bmatrix}.$$

10 References

[1] P. Vas: Sensorless Vector and Direct Torque Control, Oxford University Press, 2003.

[2] B. Bose: Modern Power Electronics and AC Drives, Prentice Hal, 2002.

[3] V. Vasic: Control of Induction Motor without Shaft Sensor, PhD Thesis, University of Belgrade, School of Electrical Engineering, Belgrade, 2001.

[4] J. Holtz: Sensorless Control of Induction Machines-With or without Signal Injection, IEEE Transaction on Industrial Electronics, Vol. 53, No 1, 2006, pp. 7 – 30.

[5] H. Kubota, K. Matsuse, T. Nakano: DSP Based Speed Adaptive Flux Observer of Induction Motor, IEEE Transaction on Industry Applications, Vol. 29, No. 2, 1993, pp. 344 – 348.

[6] H. Kubota, K. Matsuse: Speed Sensorless Field-Oriented Control of Induction Motor with Rotor Resistance Adaptation. IEEE Transaction on Industry Applications, Vol. 30, No. 5, 1994, pp. 1219 – 1224.

[7] J. Ha, S. Sul: Sensorless Field-Orientation Control of an Induction Machine by High Frequency Signal Injection, IEEE Transactions of Industry Applications, Vol. 35, No. 1, 1999, pp. 45 – 51.

[8] M. Jouili, K. Jarray, Y. Koubaa, M. Boussak: Luenberger State Observer for Speed Sensorless ISFOC Induction Motor Drives, Electric Power Systems Research, 2012, Vol. 89, pp. 139 – 147.

[9] I. M. Alsofyani, N.R.N. Idris: A Review on Sensorless Techniques for Sustainable Reliability and Efficient Variable Frequency Drives of Induction Motors, Renewable and Sustainable Energy Reviews, 2013, Vol. 24, pp. 111 – 121.

[10] A. Savoia, C. Verrelli, M. Mengoni, L. Zarri, A. Tani, D. Casadei: Adaptive flux observer for induction machines with on-line estimation of stator and rotor resistances, In Proceedings of the 15th International Power Electronics and Motion Control Conference (EPE/PEMC'12), Novi Sad, Serbia, September 2012, pp. LS7b-1.3-1 – LS7b-1.3-6.

[11] V. Vuckovic: General theory of electrical machines, Nauka, Belgrade, 2009. (In Serbian).

[12] V. Vuckovic: Electrical drives. University of Belgrade, School of Electrical Engineering, Belgrade, 1997. (In Serbian).

[13] D. W. Nowotny, T. A. Lipo: Vector Control and Dynamics of AC Drives, Clarendon Press, Oxford, 1997.